Electronic Supplementary Material (ESI) for Nanoscale.

Carbon-ZnO Alternating Quantum Dot Chains: Electrostatic Adsorption Assembly and White Light-emitting Device Application

Kai-Kai Liu, Xiao-Ming Li, Shao-Bo Cheng, Rui Zhou, Ya-Chuan Liang, Lin Dong, Chong-Xin Shan, Hai-Bo Zeng,*and De-Zhen Shen**

Table of contents in Supporting Information

8. **Figure S8.** PLE spectra of the CZA-QDC powders and fluorescence spectra of the CZA-QDC powders with different excitation wavelengths

9. **Figure S9.** (a) Fluorescence spectra of the CZA-QDC powders after different annealing temperatures. (b) The fluorescence spectra of the CZA-QDC powders in different storage times.

10. **Figure S10**. The luminescence spectra of the WLED under different driving currents.

11. **Figure S11.** The images of WLED under different driving currents.

12. **Figure S12.** A typical luminescence image of the WLED under normal lighting conditions, and the inset is the image of the UV chip coated with the CZA-QDC powders.

13. **The mole ratio between CNDs and ZnO QDs in the CZA-QDC powders**

The energy dispersive x-ray (EDX) spectroscopy was used to characterize the elemental composition of the ZnO QD powders and CZA-QDC powders. Considering that the sample will adsorb CO_2 during the measurement process, we conduct contrast experiment between pure ZnO QD powders and CZA-QDC powders. From the EDX spectrum of ZnO QD powders, the *At*% of C is 44.66%; while in the spectrum of CZD-QDC powders, the *At*% of C increases to 52.53%. The *At*% of C in the CZA-QDC powders has increased by 7.87%, which can be attributed to the addition of CNDs, as shown in Figure S6. The *At*% of Zn in CZA-QDC powders is 6.06%, we thus can conclude that the mole ratio between the carbon nanodots and ZnO QDs is about 1.3 in the CZA-QDC powders.

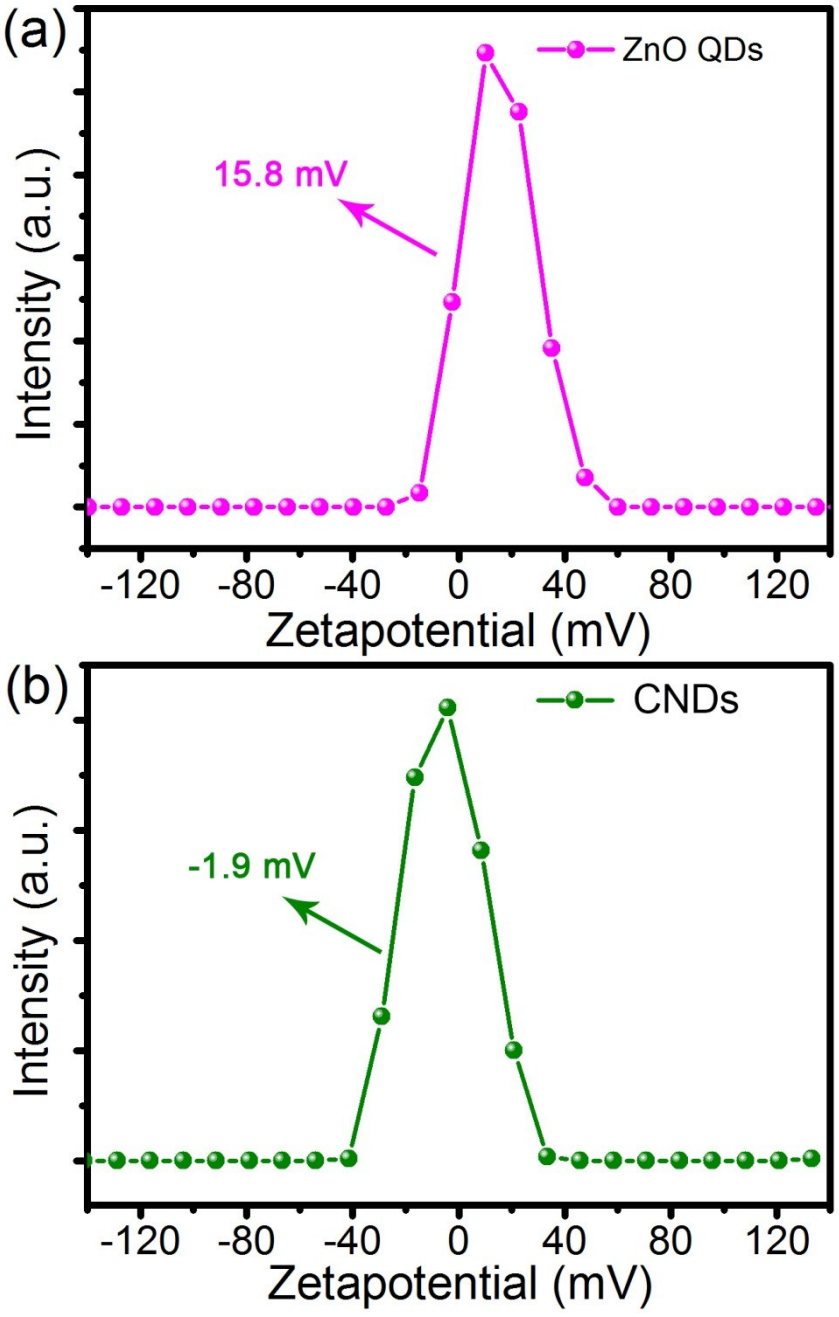

Figure S1. (a) Zetapotential of ZnO QDs. (b) Zetapotential of CNDs.

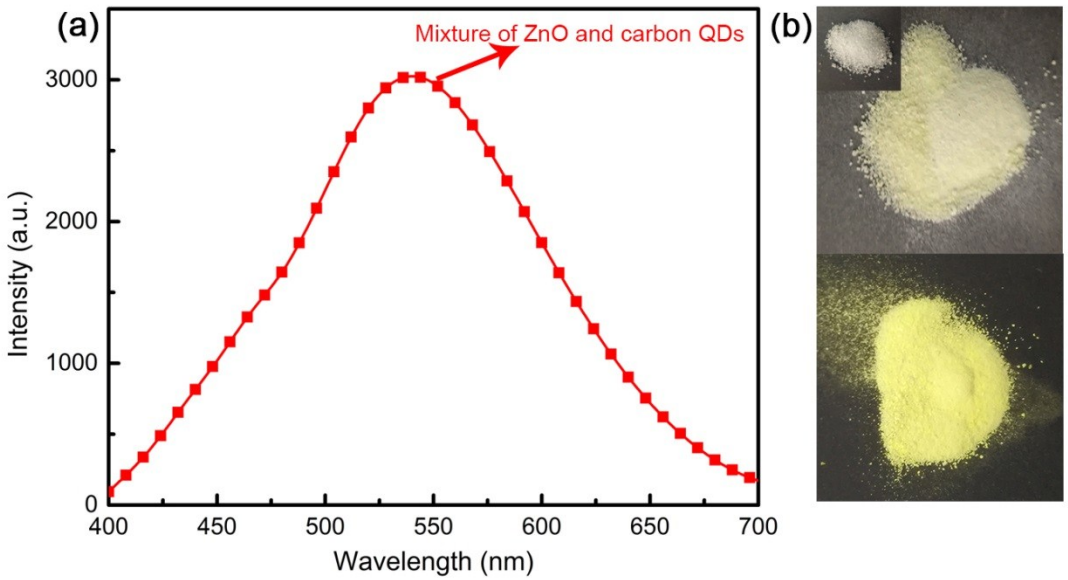

Figure S2. (a) Fluorescence spectrum of the mixture of ZnO and CNDs. (b) Photograph of the mixture of ZnO and CNDs under indoor lighting and UV illumination, the inset is the photograph of ZnO QD powders under indoor lighting.

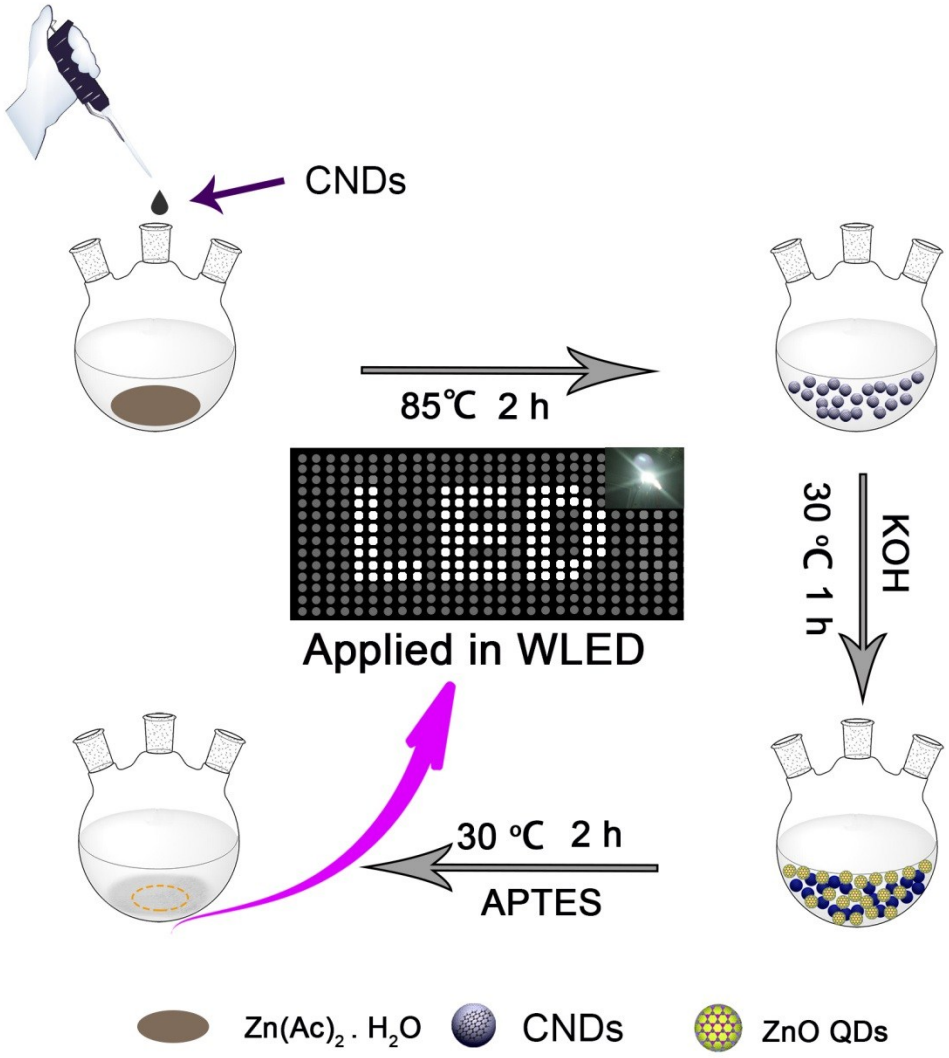

Figure S3. Schematic illustration of the synthesis process of the CZA-QDCs

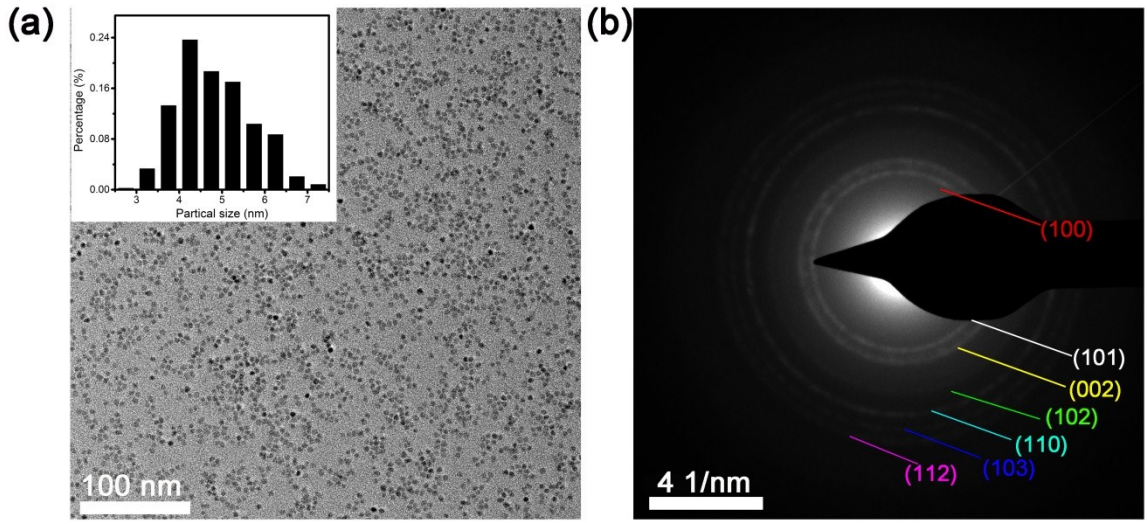

Figure S4. (a) TEM image of the ZnO QDs, and the inset shows the size distribution of the ZnO QDs. (b) Selected-area diffraction pattern of the ZnO QDs.

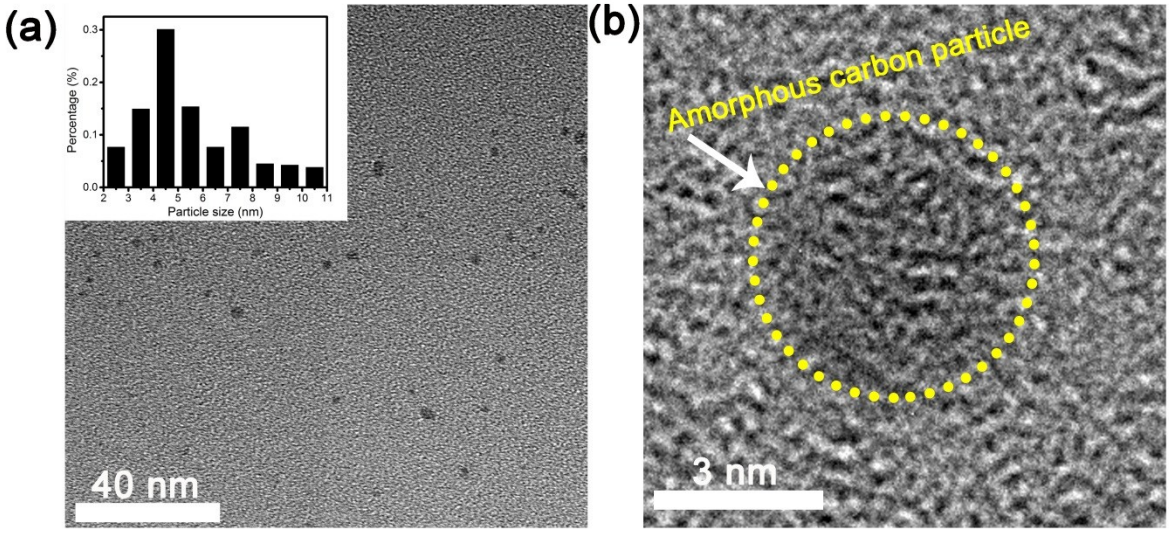

Figure S5. (a) TEM image of the CNDs, the inset is the size distribution of CNDs. (b) High-resolution TEM image of the CNDs.

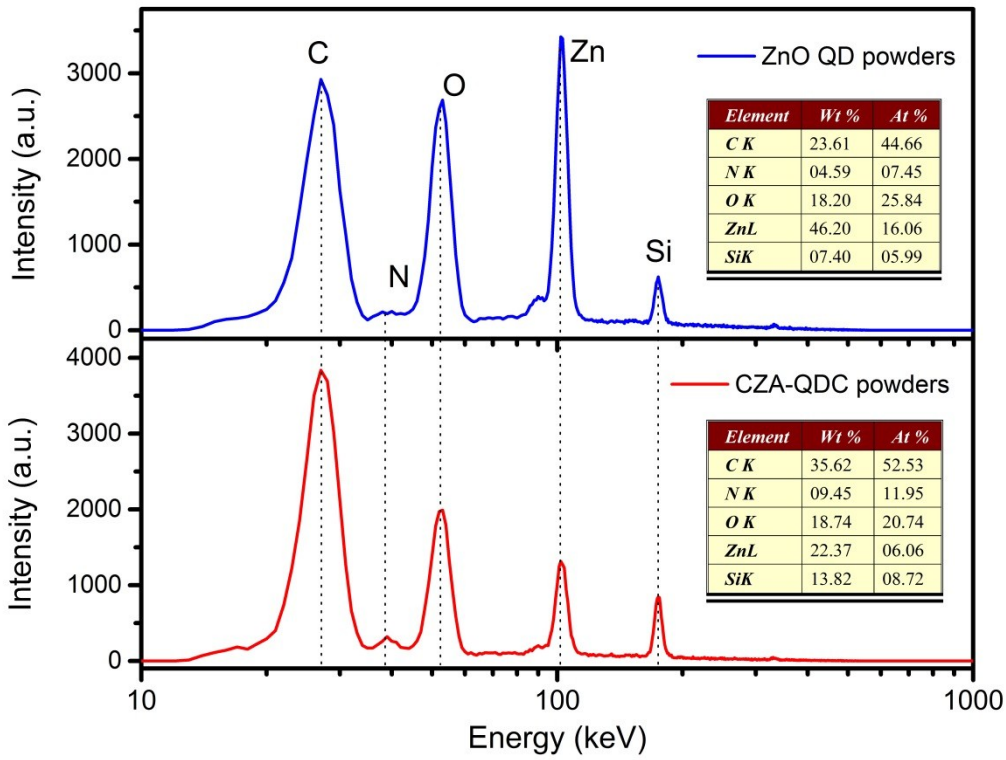

Figure S6. EDX spectra of ZnO QD powders and CZA-QDC powders

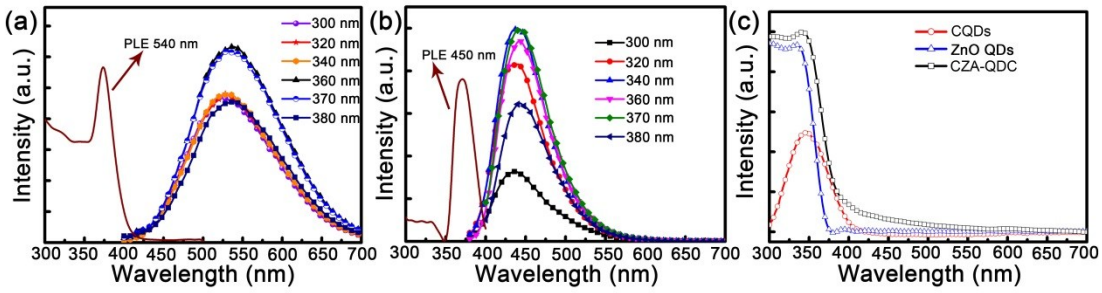

Figure S7. (a) PLE spectrum of the emission at 540 nm from the ZnO QD solution, and the fluorescence spectra of the ZnO QDs under different excitation wavelength. (b) PLE spectrum of the emission at 450 nm from the CND solution and the fluorescence spectra of the CNDs under different excitation wavelength. (c)

Absorption spectra of the CNDs, ZnO QDs and CZA-QDC solution.

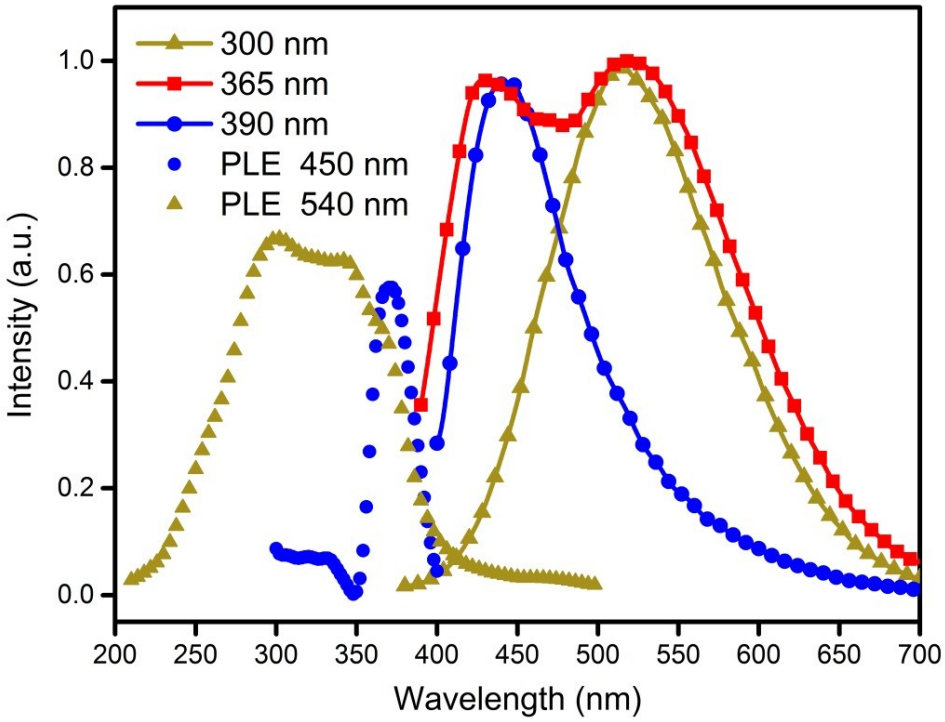

Figure S8. PLE spectra of the CZA-QDC powders and fluorescence spectra of the CZA-QDC powders with different excitation wavelengths

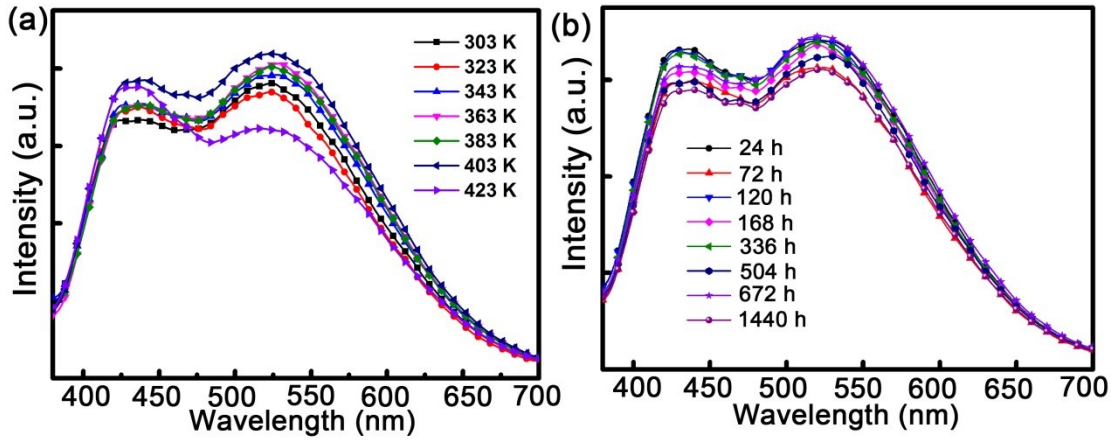

Figure S9. (a) Fluorescence spectra of the CZA-QDC powders after different annealing temperatures. (b) The fluorescence spectra of the CZA-QDC powders in different storage times.

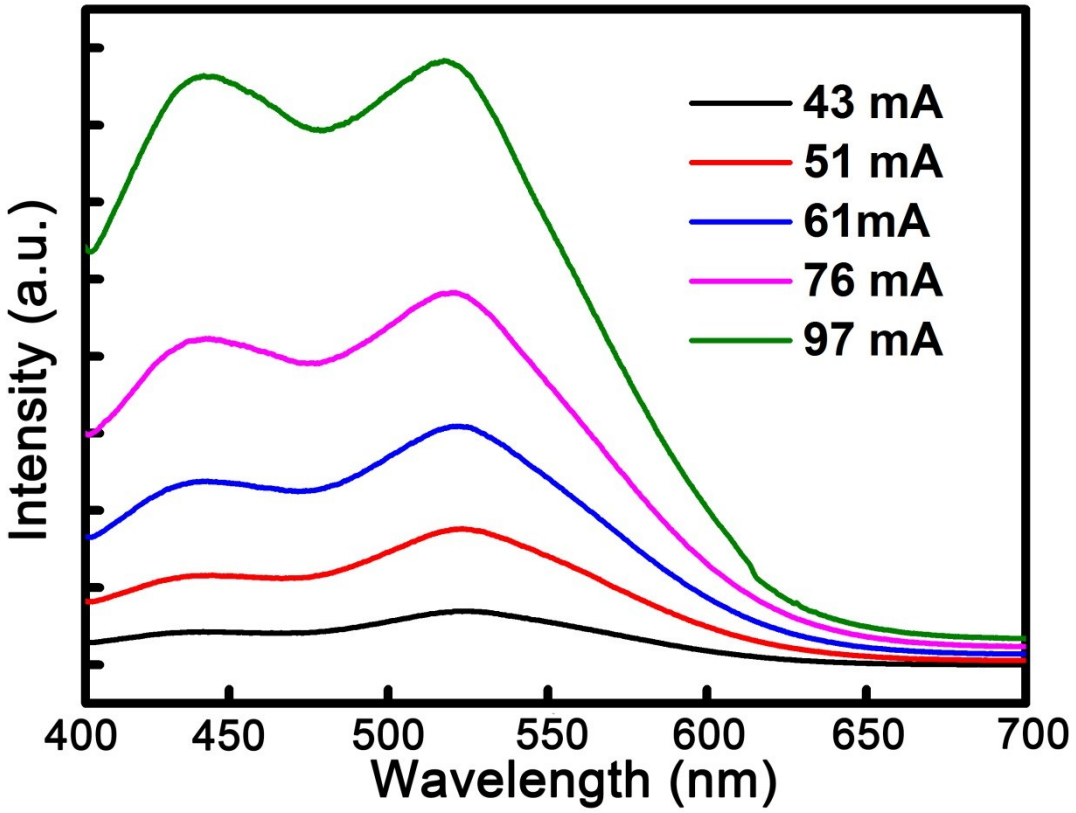

Figure S10. The luminescence spectra of the WLED under different driving currents.

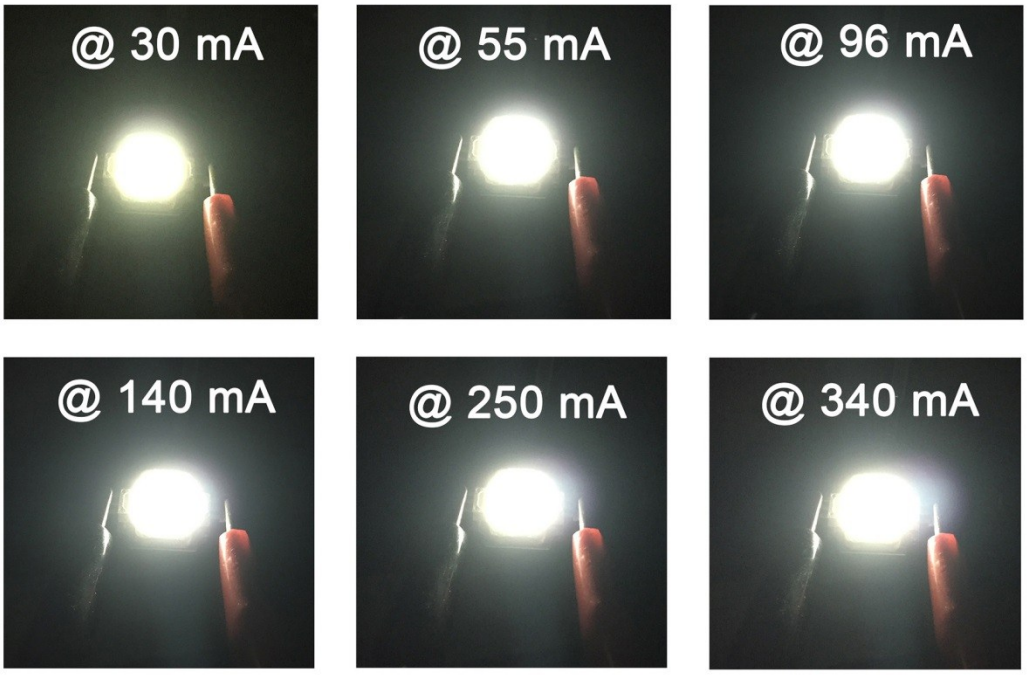

Figure S11. The images of WLED under different driving currents.

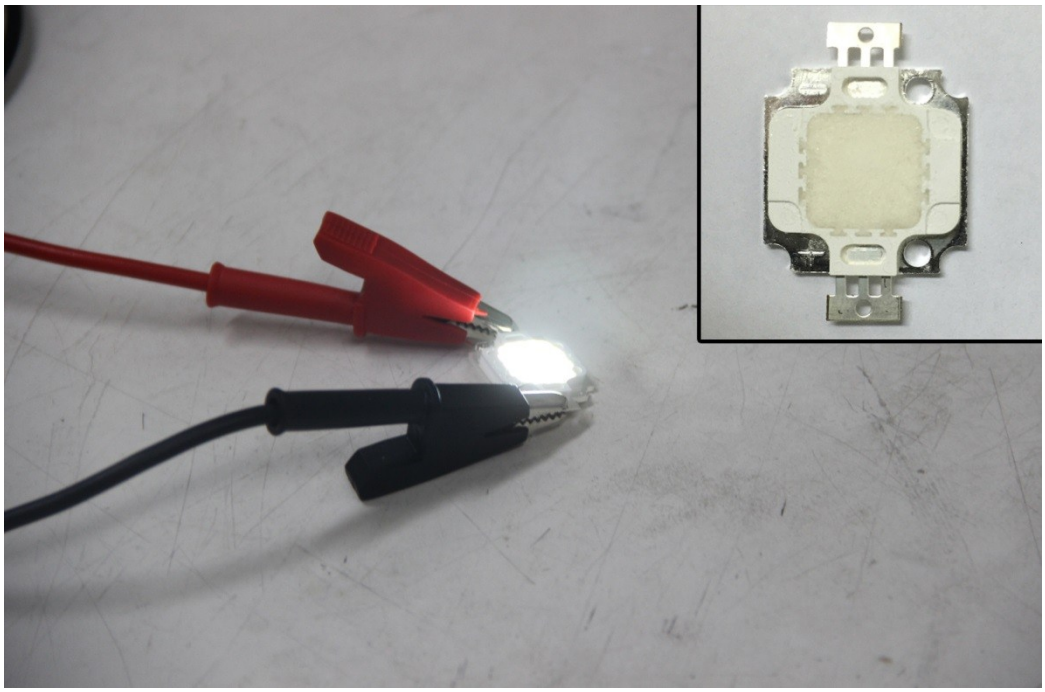

Figure S12. A typical luminescence image of the WLED under normal lighting conditions, and the inset is the image of the UV chip coated with the CZA-QDC powders.